II. Pitch-Angle Diffusion

II.1 Violation of an Adiabatic Invariant

Purely adiabatic motion, as described at length in Chapter I, characterizes the dynamical problem in which the phases φ_1, φ_2, and φ_3 are cyclic coordinates. These are the phases canonically conjugate to the fundamental action integrals $J_1 = 2\pi m_0 c|q|^{-1} M$, $J_2 = J$, and $J_3 = (q/c)\Phi$ that identify the three adiabatic invariants M, J, and Φ of charged-particle motion. Strict conservation of M, J, and Φ is only a kinematical ideal that provides the framework for understanding radiation-belt dynamics, and geophysically interesting dynamical phenomena involve violation of one or more of the invariants. Violation of an adiabatic invariant occurs in the presence of forces that vary on so short a spatial or temporal scale that particles having the same three adiabatic invariants (but different phases) respond inequivalently.

Ordinarily this means that violation of the invariant associated with the action integral J_i requires application of a force that varies abruptly on a time scale comparable to the corresponding periodicity of adiabatic motion ($2\pi/\Omega_i$). In some instances, however, spatial symmetries may preserve an invariant even if this condition on the time scale is satisfied. On the other hand, spatial variations of the force field that are abrupt on a length scale comparable to the gyroradius can violate adiabatic invariants, irrespective of the temporal scale.

A variety of geophysical processes can violate the invariants of adiabatic motion. Collisions, for example, act on a scale that is both spatially and temporally abrupt with respect to gyration, and all three of a charged particle's adiabatic invariants can be violated thereby. Electrostatic and electromagnetic plasma cyclotron waves similarly distinguish among particles having different gyration, bounce, and drift phases. Such waves are capable of violating all three adiabatic invariants. Geomagnetic micropulsations typically have frequencies comparable to particle bounce or drift frequencies, and thus can violate J and/or Φ. In many of these examples, the violation of Φ is not severe by comparison with that induced by geomagnetic sudden impulses and other storm- and substorm-associated disturbances of magnetospheric extent. Such disturbances distinguish among particles instantaneously present at different magnetic longitudes (having distinct drift phases

φ_3), but generally average over the phases φ_1 and φ_2, thereby conserving the first two adiabatic invariants.

If the force field responsible for violating the adiabatic invariant associated with an action integral J_i exhibits sufficient spatial and temporal coherence, the distribution of particles initially having in common their values of M, J, and Φ can thereby become organized with respect to the phase φ_i. Then, assuming for simplicity that only one invariant is violated, the associated dispersal of these particles with respect to the conjugate momentum $J_i/2\pi$ can be understood as a consequence of Liouville's theorem (Section I.3)[12]. The dispersal is deterministic in the sense that ΔJ_i, the change in value of J_i, is a function of φ_i; but the dispersal of a particle distribution with respect to J_i appears random if one averages over (or loses sight of) the phase φ_i. In practice, phase mixing always occurs eventually (see Introduction) because any observational instrument has a greater-than-infinitesimal bandwidth with respect to the three invariants. Particles having slightly different values of M, J, and Φ may therefore be counted as being observationally equivalent in the detector. However, since these particles have slightly different values of Ω_i, encompassing a bandwidth $\Delta\Omega_i/2\pi$, their phases φ_i will mix adiabatically on a time scale $\sim 2\pi/\Delta\Omega_i$. Phase memory persists in the distribution as the particles continue to gyrate, bounce, and drift, but this memory is hidden from an observer, to whom the particles appear to be randomly phased (see Introduction).

For this reason, an essentially complete physical description of the earth's radiation environment is provided by specifying the *phase-averaged* particle fluxes (see Introduction) in terms of M, J, Φ, and time. This suppression of the phase variables φ_i introduces an essential component of randomness that permits violation of the adiabatic invariants to be represented by *diffusion* of the particle population with respect to M, J, and/or Φ under most circumstances of interest. After phase averaging, the various elements of the particle distribution, subjected to nonadiabatic forces, usually appear to have walked randomly with respect to the violated invariants. Thus, the ultimate inability to distinguish particle phases by observation is a simplifying virtue.

Since the action variables $J_i/2\pi$ are canonical, the basic form of the diffusion equation for radiation-belt particles is

$$\frac{\partial \bar{f}}{\partial t} = \sum_{ij} \frac{\partial}{\partial J_i}\left[D_{ij}\frac{\partial \bar{f}}{\partial J_j}\right], \tag{2.01}$$

[12] Since the distribution function moves "incompressibly" through phase space in Hamiltonian mechanics [7], a narrowing of the distribution with respect to φ_i implies a broadening with respect to the J_i, and vice versa.

where $\bar{f}(\mathbf{p},\mathbf{r};t)$ is the phase-averaged particle distribution function and D_{ij} is the tensorial diffusion coefficient. For practical purposes, there are only two classes of interaction not describable in terms of (2.01). One class involves change of particle identity, *e.g.*, beta decay, electron attachment, recombination, charge exchange, inelastic capture, nuclear excitation. The other class falls under the general heading of "friction", *e.g.*, the gradual deposition of energy by energetic particles traveling through matter. Where such processes are truly important, as for the inner-zone proton population, it is necessary (and not usually difficult) to add the appropriate source and sink terms to (2.01). Although some of these non-diffusive processes are included below, the primary emphasis of the present work is on that multitude of processes under which (2.01) very adequately describes the behavior of radiation-belt particles.

It is customary in radiation-belt physics to distinguish between pitch-angle diffusion (which violates M or J, and usually both) and radial diffusion (which violates Φ). Although some diffusive processes violate all three invariants, the dichotomous viewpoint is conceptually convenient. As a rule, radial diffusion enables the radiation belts to become populated from an external source (or rearranges particles injected by an internal source), while pitch-angle diffusion causes particle loss to an atmospheric sink. There are exceptions to this rule, but it is often fruitful to think in these terms; hence the distinction between radial diffusion and pitch-angle diffusion. The present chapter is devoted to pitch-angle diffusion, which arises from a variety of mechanisms.

II.2 Collisions

Because radiation-belt particles have such high energies and low densities (see Chapter I), Coulomb collisions between them are completely negligible. Collisions with ionospheric constituents, however, contribute importantly to the ultimate demise of geomagnetically trapped radiation. Energetic particles traveling through matter (including the ionospheric medium) tend to yield their energy to free and bound ambient electrons or to the excitation of atomic nuclei. Moreover, the phenomenon of charge exchange with an ambient atom effectively removes an energetic proton from the radiation-belt population.

As noted above, processes involving *systematic* energy loss to the medium are generally not describable by (2.01). Special terms must be added to account for such *non-diffusive* effects, although the friction mechanism may simultaneously be responsible for diffusion in pitch angle. Because systematic energy loss to the medium can be interpreted as a convective flow of $\bar{f}(\mathbf{p},\mathbf{r};t)$ through adiabatic-invariant space, these

special terms have the form of the "divergence" of a non-stochastic "current" in the *Fokker-Planck equation*

$$\frac{\partial \bar{f}}{\partial t}+\sum_i \frac{\partial}{\partial J_i}\left[\left(\frac{dJ_i}{dt}\right)_v \bar{f}\right]=\sum_{ij}\frac{\partial}{\partial J_i}\left[D_{ij}\frac{\partial \bar{f}}{\partial J_j}\right], \tag{2.02}$$

in which the subscript v refers to frictional (non-stochastic) processes. Ordinarily the Fokker-Planck equation is written in the form

$$(\partial \bar{f}/\partial t)=-\sum_i [\partial(D_i' \bar{f})/\partial J_i]+\sum_{ij}[\partial^2(D_{ij}\bar{f})/\partial J_i \partial J_j], \tag{2.03a}$$

where

$$D_i'=(dJ_i/dt)_v+\sum_j(\partial D_{ij}/\partial J_j). \tag{2.03b}$$

The relationship between $\bar{f}$ and the phase-averaged flux $\bar{J}_z$ is given by (1.61), in Section I.7.

Inner-Zone Protons. An important example of non-stochastic "flow" in phase space is the deceleration of inner-zone protons ($M \lesssim 4\,\mathrm{GeV/gauss}$) by free and bound electrons in the upper ionosphere. Because the rest-mass ratio m_p/m_e is so large, the protons experience no significant range straggling or pitch-angle diffusion (see below) in traversing the medium. In other words, the equatorial pitch angle remains constant while M and J decrease systematically by virtue of energy transfer. The rate of energy transfer is obtained by means of elaborate quantum-mechanical calculations, which yield [37, 38]

$$\begin{aligned}(m_e v/4\pi q_p^2 q_e^2)(dE/dt)_v = {} & \bar{N}_e[1-\gamma^{-2}-\ln(\lambda_D m_e v/\hbar)] \\ & +\sum_i \bar{N}_i Z_i\{1-\gamma^{-2}-\ln[2m_e c^2(\gamma^2-1)/I_i]\},\end{aligned} \tag{2.04}$$

where v is the speed of the proton, and γ is its ratio of relativistic mass to rest mass. The quantities $\bar{N}_e$ and $\bar{N}_i$ are obtained by averaging the densities of free electrons (N_e) and gas molecules (N_i), each of the latter containing Z_i bound electrons, over the proton trajectory (drift shell). Since the ionospheric (or plasmaspheric) Debye length λ_D appears only logarithmically in (2.04), it may be evaluated anywhere on the drift shell (*e.g.*, where $N_e=\bar{N}_e$) without introducing substantial error. The quantity I_i has the significance of a mean excitation energy for the bound electrons; typical values of I_i, along with drift-averaged values of N_e and N_i [38], are given in Table 5 for selected drift shells on which $J=0$. These shells are identified by the McIlwain parameter L_m (see Section I.5), which equals $(B_0/B_m)^{1/3}$ in the case of particles mirroring at the magnetic equator. The major contribution to each

Table 5. Drift-Averaged Atmospheric Densities, cm^{-3}

L_m	j	$\|Z_j\|$	I_i, eV	Phase of Solar Cycle		
				Maximum	Averaged	Minimum
1.150	H	1	15	5.36×10^{3}	7.09×10^{3}	1.17×10^{4}
1.186	H	1	15	4.48×10^{3}	5.90×10^{3}	9.58×10^{3}
1.247	H	1	15	3.32×10^{3}	4.34×10^{3}	6.93×10^{3}
1.349	H	1	15	2.23×10^{3}	2.88×10^{3}	4.50×10^{3}
1.500	H	1	15	1.30×10^{3}	1.65×10^{3}	2.50×10^{3}
1.900	H	1	15	5.15×10^{2}	5.99×10^{2}	9.22×10^{2}
2.500	H	1	15	1.95×10^{2}	2.24×10^{2}	3.09×10^{2}
1.150	He	2	41	1.26×10^{6}	6.17×10^{5}	1.52×10^{5}
1.186	He	2	41	5.94×10^{5}	2.83×10^{5}	6.51×10^{4}
1.247	He	2	41	1.74×10^{5}	7.98×10^{4}	1.70×10^{4}
1.349	He	2	41	3.40×10^{4}	1.48×10^{4}	2.84×10^{3}
1.500	He	2	41	3.83×10^{3}	1.55×10^{3}	2.61×10^{2}
1.900	He	2	41	9.64×10^{1}	2.86×10^{1}	
2.500	He	2	41	2.25×10^{0}	7.51×10^{-1}	
1.150	O	8	89	4.83×10^{6}	2.41×10^{6}	8.24×10^{5}
1.186	O	8	89	1.87×10^{5}	8.41×10^{4}	1.87×10^{4}
1.247	O	8	89	9.87×10^{2}	3.77×10^{2}	5.92×10^{1}
1.349	O	8	89		2.82×10^{1}	
1.150	N_2	14	78	2.45×10^{4}	1.66×10^{4}	6.46×10^{3}
1.186	N_2	14	78	8.06×10^{1}	4.61×10^{1}	1.27×10^{1}
1.150	O_2	16	89	5.57×10^{2}	3.53×10^{2}	1.19×10^{2}
1.150	e	1		1.15×10^{5}	1.62×10^{4}	1.61×10^{4}
1.186	e	1		4.11×10^{4}	5.34×10^{3}	7.83×10^{3}
1.247	e	1		9.32×10^{3}	2.89×10^{3}	4.59×10^{3}
1.349	e	1		3.29×10^{3}	3.03×10^{3}	3.24×10^{3}
1.500	e	1		2.66×10^{3}	2.65×10^{3}	2.66×10^{3}
1.900	e	1		1.69×10^{3}	1.69×10^{3}	1.69×10^{3}
2.500	e	1		7.92×10^{2}	7.92×10^{2}	7.92×10^{2}

$\bar{N}_j$ on these drift shells occurs at the South Atlantic "anomaly" (see Section I.5), where each of the shells attains its perigee altitude under adiabatic motion.

The quantity $E|dE/dt|^{-1}$ is interpreted as an instantaneous e-folding time for the kinetic energy of a proton depositing its energy in the atmosphere. The dependence of this e-folding time on L_m is illustrated in Fig. 14 for protons having selected values of M (given in GeV/gauss) and $J=0$ [39]. At constant M and J, the "lifetime" against Coulomb deceleration thus peaks at $L_m\approx1.6$.

In view of the great magnitude of the time scales for proton energy loss (see Fig. 14), it is essential to re-examine assumptions concerning

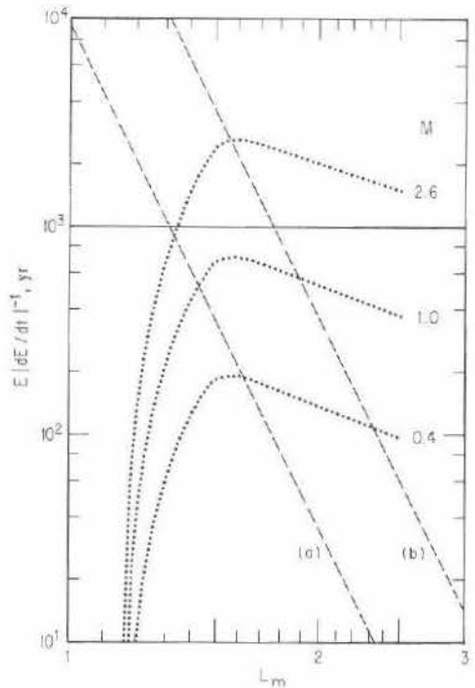

Fig. 14. Effective lifetimes against Coulomb drag (energy loss) for equatorially mirroring inner-zone protons (dotted curves) at selected values of the first invariant M, GeV/gauss. Solid curve shows corresponding time scale $-B_0/2\dot{B}_0$ for energization by present secular variation of geomagnetic dipole moment [39]. Dashed curves show roughly corresponding time scales $L^2/30D_{LL}$ for energization by inward radial diffusion (see Section III.8), assuming (a) $D_{LL}=10^{-8}L^{10}$ day^{-1} and b) $D_{LL}=10^{-9}L^{10}$ day^{-1}.

the constancy of B_0 in (1.37) when carrying out *theoretical* calculations. In fact, the present value of $\dot{B}_0(\approx-0.016$ gauss/century) leads to an instantaneous time scale $-(L/\dot{L})=-(B_0/\dot{B}_0)\sim2000$ yr for the secular contraction of adiabatic drift shells. The conservation of M and J during this secular contraction implies a secular energization of geomagnetically trapped particles. In a contracting dipole field the preservation of $M\equiv p^2y^2L^3/2m_0B_0$ and $J\equiv2LapY(y)$ implies $dy/dt=0$ and

$$\frac{1}{E}\frac{dE}{dt}=-\frac{2}{B_0}\frac{dB_0}{dt}\left[\frac{\gamma+1}{2\gamma}\right]\sim\frac{[(\gamma+1)/2\gamma]}{1000\,\text{yr}}. \tag{2.05}$$

Thus, the equatorial pitch angle remains invariant, and a nonrelativistic proton has its energy increased by a factor of e on a time scale ~1000 yr (see Fig. 14). This time scale is comparable to that for energy loss

to free and bound electrons, and so it appears that the two processes are mutually competitive for inner-belt protons [39].

Since inner-zone protons are subject, in addition, to radial diffusion over the time scales of interest, a theoretical analysis of the quasi-static profile of the inner belt is deferred to a later chapter (see Section V.7). At this point it is appropriate to discuss only the form of $(dJ_i/dt)_v$ and of its "divergence" with respect to J_i. Since $J_1 = 2\pi m_0 c|q|^{-1} M$ and $J_2 = J$, this "divergence" may be written (for a dipole field) as

$$\begin{aligned}\sum_i \frac{\partial}{\partial J_i}\left[\left(\frac{dJ_i}{dt}\right)_v \bar{f}\right] &= \frac{\partial}{\partial M}\left[\left(\frac{dM}{dt}\right)_v \bar{f}\right]_{J,\Phi} + \frac{\partial}{\partial J}\left[\left(\frac{dJ}{dt}\right)_v \bar{f}\right]_{M,\Phi} \\ &= \frac{\partial}{\partial M}\left[\left(\frac{dM}{dt}\right)_v \bar{f}\right]_{\Phi} + \frac{\bar{f}}{2M}\left(\frac{dM}{dt}\right)_v \\ &= \left(\frac{m_0}{2MB_m^3}\right)^{1/2} \frac{\partial}{\partial M}\left[\gamma^2 v\left(\frac{dE}{dt}\right)_v \bar{f}\right]_{\Phi}\end{aligned} \tag{2.06}$$

in the limit of equatorially mirroring ($J=0$) protons, for which $(dE/dt)_v$ is given by (2.04)[13]. The unidirectional flux $\bar{J}_\perp (\equiv 2m_0 M B_m \bar{f})$ is considered a function of M and Φ in (2.06) and should be evaluated at the magnetic equator, where $B = B_e$. Of course, both γ and $(dE/dt)_v$ are functions of M and Φ as well; in a dipole field the fact that $B_e = B_0 L^{-3} = (1/8\pi^3 a^6 B_0^2)|\Phi|^3$ implies

$$\gamma^2 = 1 + (2MB_0/m_0 c^2 L^3) = 1 + (M/4\pi^3 a^6 B_0^2 m_0 c^2)|\Phi|^3 \tag{2.07}$$

for particles having $J=0$. In this case the phase-averaged distribution function that satisfies (2.02) is given by

$$\bar{f} = |\Phi|^{-3}(4\pi^3 a^6 B_0^2/m_0 M)\bar{J}_\perp . \tag{2.08}$$

Coulomb energy loss for ions other than protons can be evaluated from (2.04) if q_p is replaced by the ionic charge and v interpreted as the ionic velocity[14].

Charge Exchange. For protons of much lower energy than those represented in Fig. 14, the main collisional "loss" mechanism is *charge exchange*, whereby a proton absorbs an electron from an ambient atom

[13] Note that $v(dE/dt)_v$ depends rather weakly on M, which reduces to $(\gamma^2 - 1) \times (m_0 c^2/2B_e)$ for $J=0$. It can be shown by Jacobian methods (see below) that (2.06) holds not only for $J=0$, but more generally for any constant value of $K^2 \equiv J^2/8m_0 M$.

[14] As noted above, the explicit time dependence of B_0 is potentially an important effect for the inner proton belt. The time scales illustrated in Fig. 14 apply only to the present epoch, and not to past or future centuries.

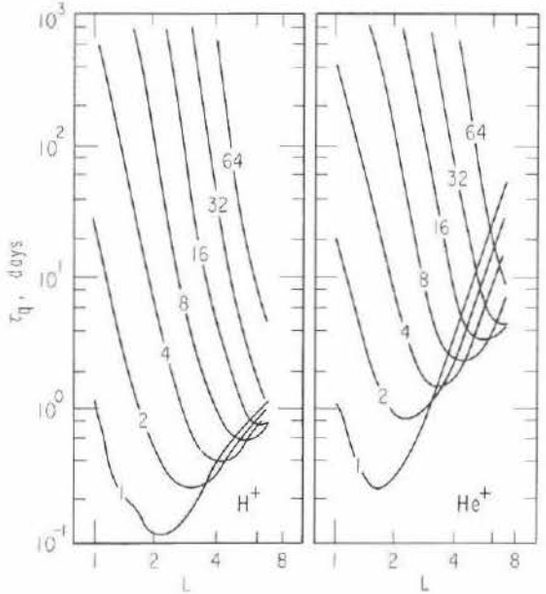

Fig. 15. Charge-exchange lifetimes against neutralization for equatorially mirroring protons (H^+) and helium ions (He^+) at selected values of M/A, MeV/gauss-nucleon [40].

and escapes from the radiation belt as an energetic hydrogen atom. This process is microscopically catastrophic (a "one-shot" interaction), and so, unlike that described by (2.04), it is best characterized by a true lifetime $\tau_q = l_q/v$, where l_q is a mean free path. Typical charge-exchange lifetimes against conversion of H^+ and He^+ ions into H^0 and He^0 atoms by the hydrogen-atom environment are illustrated in Fig. 15 [40] for an appropriate atmospheric model [41]. It is conventional to compare coincident radiation-belt fluxes of distinct ionic species at common values of E/A (kinetic energy per nucleon), where A is the number of nucleons in the ionic nucleus. According to this convention[15], first invariants M for H^+ are directly comparable with first invariants $4M$ for He^+. The particles described in Fig. 15 are nonrelativistic and have vanishing second invariants ($J=0$). The governing equation

[15] Because the conventional comparison is between ions having E/A in common at the same point in space, and therefore having v and γ in common within experimental error, the Coulomb "lifetimes" $|(d \ln E/dt)_v|^{-1}$ scale as A_j/q_j^2 according to (2.04), where the subscript j denotes the species of the energetic ion.

in the presence of simple charge-exchange losses has the form

$$\frac{d\bar{f}}{dt} \equiv \frac{\partial \bar{f}}{\partial t} + \sum_i \frac{\partial}{\partial J_i}\left[\left(\frac{dJ_i}{dt}\right)_v \bar{f}\right] - \sum_{ij} \frac{\partial}{\partial J_i}\left[D_{ij}\frac{\partial \bar{f}}{\partial J_j}\right] = -\frac{\bar{f}}{\tau_q}. \quad (2.09)$$

The charge-exchange lifetimes shown in Fig. 15 are deduced from cross sections σ [40] shown in Fig. 16, applied to a model atmosphere [41]

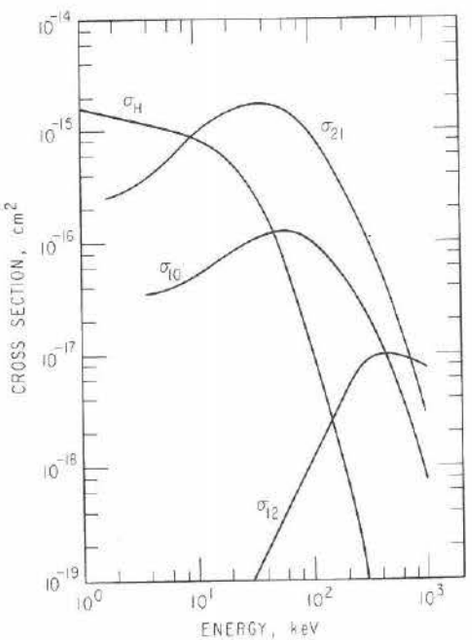

Fig. 16. Ion-energy dependence of charge-exchange cross sections in atomic-hydrogen atmosphere [40].

and model field. Evidently charge transfer is a simple loss process governed by (2.09) only for singly charged ions (with $E \lesssim 400$ keV in the case of He^+). A single cross section σ_H governs conversion of H^+ into H^0, and there are no competing channels open to radiation-belt protons. Three separate cross sections are needed to describe charge transfer in helium: σ_{10} for the neutralization of He^+ ($He^+ \rightarrow He^0$), σ_{12} for the conversion of He^+ into He^{++} (an insignificant reaction for $E \lesssim 400$ keV), and σ_{21} for the conversion of He^{++} into He^+ (the largest cross section of the three for $E \lesssim 400$ keV). Thus, in the presence of

comparable He^+ and alpha-particle (He^{++}) fluxes, it is necessary to introduce coupled transport equations for the phase-averaged distribution functions of He^+ ($\bar{f}_1$) and He^{++} ($\bar{f}_2$), *viz.*,

$$(d\bar{f}_1/dt) = -(\bar{f}_1/\tau_{10}) - (\bar{f}_1/\tau_{12}) + (\bar{f}_2/\tau_{21}) \quad (2.10a)$$

$$(d\bar{f}_2/dt) = -(\bar{f}_2/\tau_{21}) + (\bar{f}_1/\tau_{12}). \quad (2.10b)$$

Except for the possible reconversion of energetic H^0 into H^+ deep within the atmosphere in the course of precipitation (see Section II.7), no such cross coupling occurs in the description of proton or electron radiation belts. This lack of cross coupling is a welcome simplification for these two major constituents of the geomagnetically trapped radiation.

Pitch-Angle Diffusion. In addition to atmospheric deceleration, radiation-belt *electrons* undergo both *pitch-angle diffusion* and *range straggling* to a significant degree. These latter two effects arise because the mass of a radiation-belt electron is equal (apart from relativistic effects) to the mass of the atomic or plasma electrons with which it collides. The result is that deflection (pitch-angle scattering) becomes comparable in importance with energy loss. Moreover, the energy lost in an individual collision strongly depends on the scattering angle, which is a random variable. Thus, atmospheric collisions cause radiation-belt electrons to diffuse not only in pitch-angle cosine (x) but also in energy with respect to the mean value of $(dE/dt)_v$. This latter phenomenon (energy diffusion) is known as *range straggling*, because (in nuclear-physics experimentation) it permits the constituent particles of a monoenergetic beam to traverse statistically varying total path lengths before coming to rest in some material medium. For radiation-belt electrons, range straggling has the effect of smoothing the energy spectrum, which typically arises from a relatively unstructured source spectrum anyway. Thus, range straggling is usually neglected altogether.

In this and other problems for which third-invariant violation is unimportant, the variables E and x (kinetic energy and pitch-angle cosine) are usually more convenient than M and J. The corresponding diffusion matrix

$$\tilde{\mathbb{D}} \equiv \begin{pmatrix} D_{EE} & D_{Ex} \\ D_{xE} & D_{xx} \end{pmatrix} \quad (2.11)$$

is diagonal because, in individual collisions, ΔE and Δx are statistically uncorrelated; the change in energy is an *even* function of the change in x. Since the ensemble average $\langle \Delta E \Delta x \rangle$ therefore vanishes, so do the off-diagonal components of (2.11).

In general, the transformation of (2.01) and (2.02) from the set of action variables J_i to some set of new variables Q_j requires evaluation of the Jacobian [5] $G(J_i;Q_j)\equiv\det(\partial J_i/\partial Q_j)$. The diffusion operator then has the property that

$$\sum_{ij}\frac{\partial}{\partial J_i}\left[D_{ij}\frac{\partial\bar{f}}{\partial J_j}\right]=\frac{1}{G}\sum_{ij}\frac{\partial}{\partial Q_i}\left[G\tilde{D}_{ij}\frac{\partial\bar{f}}{\partial Q_j}\right]. \tag{2.12}$$

In a dipole field it is easy to calculate the Jacobian $G(M,J;E,x)$, where $M=p^2y^2L^3/2m_0B_0$ and $J=2LapY(y)$. According to (1.30), the function $Y(y)$ has the property that $Y(y)-yY'(y)=2T(y)$. The energy and momentum are related as in (1.60), and $x^2+y^2=1$. The partial derivatives needed for calculating $G(M,J;E,x)$ are

$$(\partial M/\partial E)_x=2mM/p^2 \tag{2.13a}$$

$$(\partial M/\partial x)_E=-2xM/y^2 \tag{2.13b}$$

$$(\partial J/\partial E)_x=(2mLa/p)Y(y) \tag{2.13c}$$

$$(\partial J/\partial x)_E=-(2LapxY'(y)/y^2)yY'(y), \tag{2.13d}$$

and it follows that

$$G(M,J;E,x)=(4\gamma pL^4a/B_0)xT(y). \tag{2.14}$$

Moreover, the "divergence" of the non-stochastic "current" introduced in (2.02) may be transformed to read

$$\sum_i\frac{\partial}{\partial J_i}\left[\left(\frac{dJ_i}{dt}\right)_v\bar{f}\right]=\frac{1}{G}\sum_i\frac{\partial}{\partial Q_i}\left[G\left(\frac{dQ_i}{dt}\right)_v\bar{f}\right], \tag{2.15}$$

and so the Fokker-Planck equation for radiation-belt particles subject only to atmospheric scattering (radial diffusion explicitly ignored) is

$$\frac{\partial\bar{f}}{\partial t}=-\frac{1}{\gamma p}\frac{\partial}{\partial E}\left[\gamma p\left(\frac{dE}{dt}\right)_v\bar{f}\right]_x+\frac{1}{xT(y)}\frac{\partial}{\partial x}\left[xT(y)D_{xx}\frac{\partial\bar{f}}{\partial x}\right]_E+\frac{1}{\gamma p}\frac{\partial}{\partial E}\left[\gamma pD_{EE}\frac{\partial\bar{f}}{\partial E}\right]_x. \tag{2.16}$$

The first term of (2.16) represents a non-stochastic (mean) energy loss to the atmosphere, as described by (2.04). The second term represents pitch-angle diffusion, and the associated transport coefficient is given [42] by

$$D_{xx}=\sum_j\langle(\pi/2x^2)vN_j[x^2-1+(B_e/B)]\times\int_{-1}^{+1}\{2[x^2-1+(B_e/B)](1-\cos\theta)^2+(1-x^2)\sin^2\theta\}(d\sigma_j/d\Omega)d(\cos\theta)\rangle \tag{2.17}$$

where $d\sigma_j/d\Omega$ is the differential cross section for an energetic electron incident on atmospheric constituent j at scattering angle θ in the "laboratory" frame. Debye shielding is considered in the specification of $d\sigma_j/d\Omega$. The third term of (2.16) represents range straggling (diffusion with respect to energy).

The derivation of (2.17) is straightforward. If an electron initially traveling in the $\hat{\mathbf{z}}$ direction with local pitch angle α relative to $\mathbf{B}$ (which lies locally in the xz plane) is scattered through an angle θ, the resulting change in its value of $\cos\alpha$ is

$$\Delta\cos\alpha=\cos\alpha(\cos\theta-1)+\sin\alpha\sin\theta\cos\varphi, \tag{2.18}$$

where φ is the azimuthal coordinate about the direction of $\hat{\mathbf{z}}$. Since $d\sigma_j/d\Omega$ is independent of φ, the expected value of $2(\Delta\cos\alpha)^2$ is $2\cos^2\alpha\times(1-\cos\theta)^2+\sin^2\alpha\sin^2\theta$. In terms of the equatorial pitch angle $\cos^{-1}x$, one obtains $\sin^2\alpha=1-\cos^2\alpha=(1-x^2)(B/B_e)$. It follows that

$$(\Delta x)^2=(B_e/xB)^2\cos^2\alpha(\Delta\cos\alpha)^2. \tag{2.19}$$

Finally, the diffusion coefficient D_{xx} is defined as *half* the rate at which $(\Delta x)^2$ grows with time.

The factor of one-half that enters the definition of D_{xx} can be understood in terms of a simplified prototype diffusion equation of the form

$$\partial f/\partial t=D_{\xi\xi}(\partial^2f/\partial\xi^2), \tag{2.20}$$

which applies in one-dimensional problems for which $D_{\xi\xi}$ is constant with respect to the rectilinear coordinate ξ. The use of (2.20) is chosen over (2.16) for illustrative purposes only because (2.20) is satisfied by the simple unit-normalized Green's function

$$f(\xi,t)=(2\pi a^2)^{-1/2}\exp[-(\xi-\xi_0)^2/2a^2], \tag{2.21}$$

where a is a function of time and measures the "width" of the distribution in the sense that

$$a^2=\int_{-\infty}^{+\infty}(\xi-\xi_0)^2f(\xi,t)d\xi. \tag{2.22}$$

Direct application of (2.20) implies that

$$D_{\xi\xi}=\frac{d}{dt}\left(\frac{a^2}{2}\right), \tag{2.23}$$

as indicated. Moreover, the distribution $f(\xi,t)$ given by (2.21) becomes the Dirac function $\delta(\xi-\xi_0)$ in the limit $a=0$. In view of (2.22), the quantity a^2 also represents the net mean-square migration of an individual particle (averaged over the ensemble) from the point $\xi=\xi_0$; the elapsed time of this random migration is $a^2/2D_{\xi\xi}$. This simple illustration epitomizes a general principle that is extremely useful in the calculation of diffusion coefficients from dynamical information. Of course, the metric in (2.16) is not as simple as that in (2.20), and so the Green's function is not easily identified. The basic relationship (between a diffusion coefficient and the ensemble-averaged square of the random migration with respect to a kinematical variable) holds true nevertheless.

Inner-Zone Electrons. Even with the inclusion of Debye shielding, the differential Coulomb cross section $d\sigma_j/d\Omega$ is strongly peaked in favor of forward scattering ($\theta \ll 1$). It follows that the mean value of $(1-\cos\theta)^2$ in (2.17) is *much* smaller than that of $\sin^2\theta$. The distribution of terrestrial atmosphere causes the bulk of the scattering in (2.17) to occur near the

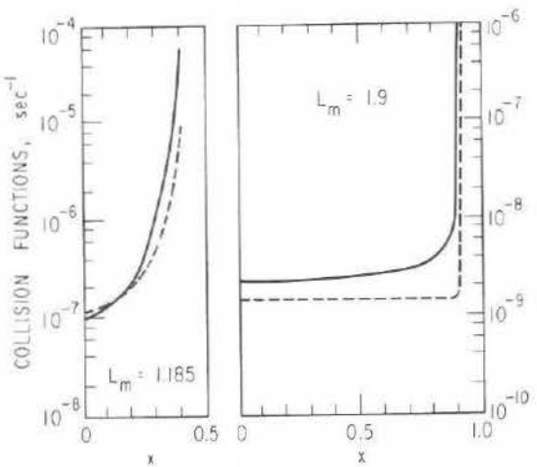

Fig. 17. Magnitudes of $-(v/m_0c^3)(dE/dt)_v$ (solid curve) and $(2p^3/\gamma m_0^3c^3y^2)D_{xx}$ (dashed curve) for inner-zone electrons subjected solely to atmospheric collisions [42].

mirror points, *i.e.*, where $B\approx B_m$. Moreover, the mirror points must not lie too deep in the atmosphere at any longitude if the phase-averaged treatment explicit in (2.01), (2.02), (2.04), (2.16), and (2.17) is to have any meaning. Other methods of analysis, preserving φ_3 as a variable,

must be employed unless $2\pi D_{xx} \ll |\Omega_3|$ and $2\pi|(dE/dt)_v| \ll |\Omega_3|E$. Granting these conditions, it is clearly permissible to neglect the term $2[x^2-1+(B_e/B)](1-\cos^2\theta)$ in (2.17) by comparison with $(1-x^2)\sin^2\theta$. The main energy dependence both of $(dE/dt)_v$ and of $d\sigma_j/d\Omega$ can be factored out, leaving the quantities $-(v/m_0c^3)(dE/dt)_v$ and $(2p^3/\gamma m_0^3c^3y^2)D_{xx}$ that are plotted [42] against x in Fig. 17 for selected values of L_m in a model atmosphere. The plotted functions, whose variations with energy are extremely weak, are evaluated here for $E\approx 1.5$ MeV. Both functions have the dimension of frequency.

Figure 17 illustrates a sharp distinction at $L_m=1.9$ between electrons for which $x \lesssim x_c \approx 0.9$ and those for which $x \gtrsim x_c$. The former are scattered almost negligibly on time scales for which the latter experience virtually immediate absorption by the atmosphere. Equatorial pitch angles for which $|x|>x_c$ are therefore said to constitute an atmospheric *loss cone* in momentum space. In mathematical terms, the coordinates $x=\pm x_c$ represent perfectly absorbing boundaries at which $\bar{f}$ is forced to vanish. Energy loss and pitch-angle diffusion satisfy the conditions $2\pi|(dE/dt)_v| \ll |\Omega_3|E$ and $2\pi D_{xx} \ll |\Omega_3|$ extremely well for $|x|<x_c$ at $E\sim 1$ MeV, thereby justifying the phase-averaged approach. The ultimate sink for inner-zone radiation, however, is quite localized at the South Atlantic "anomaly" (see Section I.5), where drifting particles having $x\approx x_c$ must dip deep into the atmosphere to find their mirror-field intensity B_m.

A rough estimate for the loss-cone angle $\cos^{-1}x_c$ can be obtained by postulating total absorption at altitude $h(\approx 0.02a)$ and displacement of the dipole by $r_0(\approx 0.07a)$ perpendicular to its axis. This eccentricity of the dipole plays an important role in cutting off the inner zone. The indicated parameters predict that

$$1-x_c^2 \approx [(a+h)/La]^3[1+3r_0(La)^{-1/2}(a+h)^{-1/2}] \div [4-(3/La)(a+h)-3r_0(La)^{-3/2}(a+h)^{1/2}]^{1/2} \qquad (2.24)$$

as a function of L. This formula yields $x_c\approx 0.940$ at $L=1.9$ (*cf.* Fig. 17), $x_c\approx 0.567$ at $L=1.185$, and $x_c=0$ at $L\approx 1.085$. Thus, the function $\bar{f}$ should vanish for all pitch angles if $L\lesssim 1.085$; in fact, a true South American anomaly accidentally near the eccentric-dipole "anomaly" raises the lower boundary of the inner zone to $L=1.10$, approximately. According to Fig. 17, the loss cone is a poorly defined feature at $L_m=1.185$, and so this simplifying concept is inapplicable there. The loss cone, however, *is* sharply defined over most of the magnetosphere (at least for $L\gtrsim 1.9$, according to Fig. 17), and is known to play an essential role in the dynamics of geomagnetically trapped radiation.

II.3 Wave-Particle Interactions

The atmosphere alone is quite incapable of accounting for the decay rates observed following temporary enhancements of the electron flux beyond $L \approx 1.25$ (see Chapter IV). The situation is indeed extreme at $L \gtrsim 4$, where storm-associated enhancements of the flux at $E \sim 0.5$ MeV characteristically decay by a factor of e on a time scale ~ 5 days [43]; *in situ* deceleration and pitch-angle scattering into the loss cone, if caused solely by collisions with the tenuous atmosphere, would require thousands of years to produce the same amount of decay. The discrepancy is qualitatively similar for outer-belt protons, although the observational data are considerably less extensive than for electrons. It is therefore natural to invoke non-collisional mechanisms for pitch-angle scattering. These mechanisms are classified under the generic term *wave-particle interactions*.

Magnetospheric waves may arise from a variety of sources. Some waves may enter the magnetosphere from the turbulent magnetosheath (see Introduction) [44]. Waves known as *whistlers* originate from lightning discharges in the atmosphere. Whistlers propagate in a plasma wave mode that can also conduct VLF (very low frequency, 3—30 kHz) radio transmissions through the magnetosphere. Man-made (Morse) signals often trigger new VLF emissions in the magnetosphere, as illustrated in Fig. 18. Moreover, plasma instabilities in the whistler (electromagnetic electron-cyclotron) and other wave modes constitute a prodigious magnetospheric source of wave energy. The VLF phenomenon known as *chorus* (see Fig. 18) apparently arises from one such instability. Other plasma instabilities may give rise to waves known as continuous (Pc) and irregular (Pi) *geomagnetic micropulsations*, which are commonly observed on the ground and in space at frequencies from ~ 2 mHz to ~ 1 Hz. A summary [4, 47] of the magnetospherically important frequency classifications is provided in Table 6.

Table 6. Classification of Magnetospheric Signals

Name	Frequency	Name	Period or Rise Time
SHF	3—30 GHz	Pc 1	$2\pi/\omega = 0.2$—5.0 sec
UHF	0.3—3.0 GHz	Pc 2	$2\pi/\omega = 5$—10 sec
VHF	30—300 MHz	Pc 3	$2\pi/\omega = 10$—45 sec
HF	3—30 MHz	Pc 4	$2\pi/\omega = 45$—150 sec
MF	0.3—3.0 MHz	Pc 5	$2\pi/\omega = 150$—600 sec
LF	30—300 kHz		
VLF	3—30 kHz	Pi 1	$\tau_r = 1$—40 sec
ELF	3—3000 Hz	Pi 2	$\tau_r = 40$—150 sec
ULF	$\lesssim 3$ Hz	sc, si	$\tau_r \sim 300$ sec

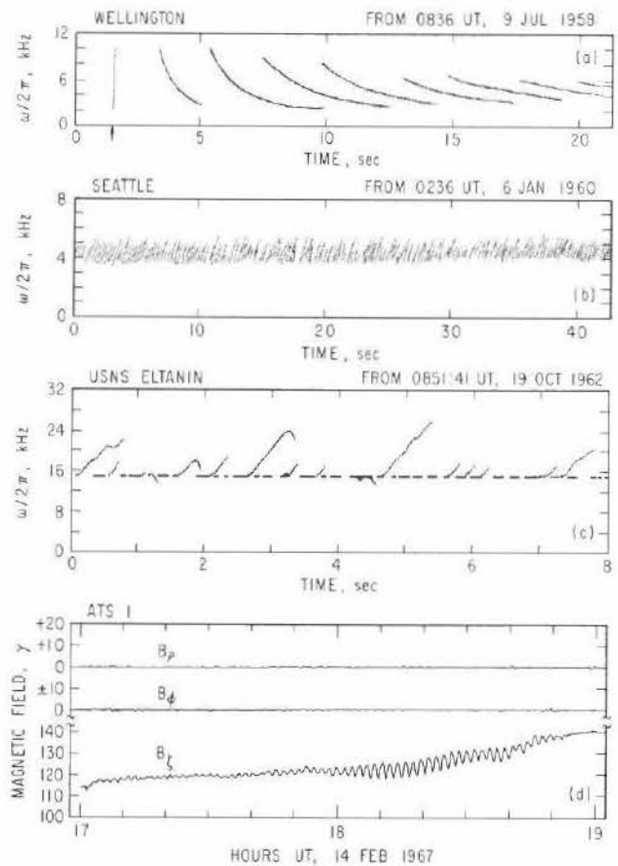

Fig. 18. Examples of magnetospheric wave phenomena observed at $r = a$ [45] and $r = 6.6a$ [46]: (a) multiple-hop whistler initiated by nearby lightning stroke (arrow) and reflected between conjugate points along a single magnetospheric path; (b) chorus, characterized by elements of sharply rising frequency; (c) rising and falling VLF emissions triggered by Morse-code transmission from NAA ($\omega/2\pi = 14.7$ kHz, $\Lambda = 56°$) and detected by mobile station at $\Lambda \approx 50°$ in the South Atlantic; (d) coherent Pc-4 micropulsation ($\omega/2\pi \sim 10^{-2}$ Hz) observed at synchronous altitude in the compressional (ζ) component, but absent in the transverse (ρ and φ) components relative to the unperturbed **B** field there.

Not all magnetospheric waves and disturbances can interact effectively with trapped particles; each trapped particle exhibits the three fundamental periodicities of adiabatic motion, and so tends to suppress (filter out) spectral components of applied forces that are distant in frequency from its natural resonances. Thus, trapped particles yield

a net diffusive response to forces that have spectral power within a narrow band about some natural resonance frequency in the frame of the particle's adiabatic motion. The width of the passband is determined by the duration of interaction, according to the classical analogue of Heisenberg's uncertainty principle. More specifically, the bandwidth $\Delta\omega$ is equal to $2\pi/\tau$, where τ is the interaction time. The interaction time may be limited by the duration of a wavelike signal or noise burst, by the time required for a particle to traverse a spatially limited region of wave activity, by temporal variation of the wave frequency required by a particle for resonance, or (more generally) by the eventual breakdown of phase coherence between a particle and the Fourier component of the wave spectrum with which it is resonant.

To the extent that the wave spectrum is smooth (structureless) over a bandwidth $\sim 2\pi/\tau$ about a resonance frequency, the interaction is truly resonant in the sense that the "line shape" resembles a Dirac delta function. More generally, the particle accepts a Lorentz-weighted mean of the wave-spectral density over a bandwidth $\Delta(\omega/2\pi)=1/\tau$ about the resonance frequency[16].

In the interest of completeness, Table 6 includes such disturbances as stormtime sudden commencements and magnetic impulses that are only vaguely wavelike in character. More precisely, the "wavelengths" associated with such disturbances are comparable in size to the magnetosphere itself. Since their time scales are so long ($\sim$ minutes), these disturbances violate only the third invariants of radiation-belt particles; such processes are considered in Chapter III. The present chapter is concerned with processes that violate either or both of the first two invariants.

II.4 Bounce Resonance

A force field can violate the second invariant (while preserving the first) through a resonant interaction with the bounce motion of a trapped particle [48]. A force $f_{\|}(s,t)$ that perturbs the bounce motion could typically originate from a compressional (magnetosonic) micropulsation, in which case $f_{\|}=-(M/\gamma)(\partial b_{\|}/\partial s)$, or from an electrostatic wave ($f_{\|}=q_j e_{\|}$). The field perturbations **b** and **e** are understood to project

[16] Violation of an adiabatic invariant is the classical analogue of the breakdown of Ehrenfest's theorem in quantum mechanics. This theorem holds that the quantum numbers of a particle, as given by the action integrals of its quasi-periodic motions in the old (Bohr-Sommerfeld) quantum theory, do not change by as much as a unit of h if the applied force field varies only on a sufficiently long time scale. Forces violating this condition lead to diffusion with respect to the classical adiabatic invariants.

nonvanishing components $b_{\|}\equiv\mathbf{b}\cdot\hat{\mathbf{B}}$ and $e_{\|}\equiv\mathbf{e}\cdot\hat{\mathbf{B}}$ along the unperturbed **B** field. If the normal (to $\hat{\mathbf{B}}$) components of **b** and **e** are confined to the azimuthal ($\hat{\boldsymbol{\varphi}}$) and meridional ($\hat{\boldsymbol{\varphi}}\times\hat{\mathbf{B}}$) directions, respectively, then bounce resonance will not contribute to radial diffusion in an azimuthally symmetric **B** field.

In this case only the second invariant is violated and the governing equation of motion [3] is

$$(dp_{\|}/dt)+(M/\gamma)(\partial B/\partial s)=f_{\|}(s,t) \tag{2.25}$$

where $p_{\|}=\gamma m_0 v_{\|}=\gamma m_0\dot{s}$. Since the unperturbed geomagnetic field **B** is taken to be static, it follows that

$$dw/dt=(p_{\|}/m_0)f_{\|}(s,t), \tag{2.26}$$

where $w=(p_{\|}^2/2m_0)+MB=p^2/2m_0$. The oscillatory force $f_{\|}(s,t)$ thus threatens to alter the particle's energy, leaving M and Φ invariant. This is equivalent to the violation of J only, and the relevant Jacobian is

$$G(M,J,\Phi;M,w,\Phi)=(\partial J/\partial w)_{M,\Phi}=4La(m_0/p)T(y) \tag{2.27}$$

if **B** is given by (1.16), *i.e.*, for a dipole field.

The oscillatory force $f_{\|}(s,t)$ is conveniently represented as a superposition of Fourier components applicable to the time interval $0<t<\tau$. This means that

$$f_{\|}(s,t)=\sum_{n=1}^{\infty} f_n\cos(k_{\|}s-\omega_n t+\psi_n), \tag{2.28}$$

where $\omega_n=2\pi n/\tau$, $k_{\|}(\mathbf{k}\cdot\hat{\mathbf{B}})$ is the parallel wavenumber corresponding to frequency $\omega_n/2\pi$, and ψ_n is the corresponding phase (ultimately a random variable) of the wavelike Fourier component. Each component contributes $(1/2)f_n^2$ to the mean-square force perturbation $\langle[f_{\|}(s,t)]^2\rangle$, and this contribution resides in a frequency interval $\Delta(\omega/2\pi)=\tau^{-1}$. It is therefore appropriate to introduce the spectral density

$$\mathscr{F}_{\|}(\omega_n/2\pi)\equiv(\tau/2)f_n^2 \tag{2.29}$$

as an optimal characterization of the force field $f_{\|}(s,t)$. Moreover, by virtue of (2.29), each Fourier component acts separately from the others.

The unperturbed bounce motion may be represented

$$s(t)\approx(px/m\Omega_2)\sin(\Omega_2 t+\varphi_2) \tag{2.30}$$

for particles having $x^2\ll 1$ (see Section I.4). It follows from (2.26)—(2.30) that

$$\Delta w\approx(px/m_0)\,\mathrm{Re}\sum_{n=1}^{\infty}\int_0^{\tau}\cos(\Omega_2 t+\varphi_2) \times f_n\exp[i(k_n px/m\Omega_2)\sin(\Omega_2 t+\varphi_2)-i\omega_n t+i\psi_n]\,dt\,. \tag{2.31}$$

If τ is interpreted as a large (ultimately infinite) integral number (N) of bounce periods $2\pi/\Omega_2$, then it follows that $\omega_n=(n/N)\Omega_2$ and

$$\Delta w \approx (p\,x/m_0)\,\tau \sum_{l=-\infty}^{+\infty} (l/z_l)\,J_l(z_l)\cos(l\varphi_2+\psi_{lN})\,f_{lN} \tag{2.32}$$

where $z_l \equiv k_{lN}\,px/m\Omega_2$ and J_l denotes the Bessel function of order l.

In the evaluation of $D_{ww}\equiv(1/2\tau)\langle(\Delta w)^2\rangle$, where the angle brackets denote the ensemble average over the phases φ_2 and ψ_{lN}, the cross terms vanish and the result is

$$D_{ww} \approx (p\,x/m_0)^2 \sum_{l=1}^{\infty} (l/z_l)^2\,J_l^2(z_l)\,\mathscr{F}_{\|}(l\,\Omega_2/2\pi)\,. \tag{2.33}$$

Since $(\partial w/\partial x)_{M,L}=2\,M\,B_0\,x/L^3\,y^4$, it is logical to define a diffusion coefficient

$$\begin{aligned} D_{xx} &= [(\partial w/\partial x)_{M,L}]^{-2}\,D_{ww} \\ &\approx (L^3\,y^6/2\,m_0\,M\,B_0) \sum_{l=1}^{\infty} (l/z_l)^2\,J_l^2(z_l)\,\mathscr{F}_{\|}(l\,\Omega_2/2\pi)\,. \end{aligned} \tag{2.34}$$

The corresponding diffusion equation

$$\frac{\partial \bar{f}}{\partial t} = \frac{y^3}{x\,T(y)}\,\frac{\partial}{\partial x}\left[\frac{x\,T(y)}{y^3}\,D_{xx}\,\frac{\partial \bar{f}}{\partial x}\right]_{M,L} \tag{2.35}$$

is constructed from the canonical formalism by inserting the Jacobian $G(M,J;M,x)=(\partial J/\partial w)_{M,L}(\partial w/\partial x)_{M,L}=(8am_0MB_0/L^2)(x/py^4)\,T(y)$ in (2.12). The diffusion coefficient D_{xx} displays a strongly inverse dependence on $x^2(\equiv 1-y^2)$, if only because of the factor y^6. In addition, the Bessel functions act to suppress D_{xx} for particles that mirror beyond a "wavelength" from the equator, *i.e.*, for $z_l \gtrsim l$. This justifies the approximation, inherent in (2.30), that bounce resonance acts principally on particles having $x^2 \ll 1$.

If the origin for $f_{\|}(s,t)$ is a spectrum of compressional (magnetosonic) micropulsations, then (in a cold plasma) the relevant dispersion relation is $\omega=c_A k$, where c_A is the Alfvén speed [49]. In this case it is found that $z_l=l(k_{\|}/k)(p\,x/m\,c_A)$ and that $b_{\|}=(k_\perp/k)b$. Since $f_{\|}(s,t)=-(M/\gamma)(\partial b_{\|}/\partial s)$, the spectral density $\mathscr{F}_{\|}(\omega/2\pi)$ has the property that

$$\mathscr{F}_{\|}(\omega/2\pi)=(M/\gamma)^2\,k_{\|}^2\,\mathscr{B}_{\|}(\omega/2\pi) \tag{2.36}$$

where $\mathscr{B}_{\|}(\omega/2\pi)$ is the spectral density of the magnetic-field perturbation $b_{\|}$. It is tacitly understood that (2.34) represents an average over the direction of propagation $\hat{\mathbf{k}}$, weighted according to the relative contribution of each $\hat{\mathbf{k}}$ to $\mathscr{B}_{\|}(\omega/2\pi)$.

Alternatively, if the oscillating force $f_{\|}(s,t)$ arises from a spectrum of electrostatic waves, then the force is given by $f_{\|}(s,t)=-q(\partial\varphi/\partial s)$, where $\varphi(s,t)$ is the oscillating electrostatic potential. For this situation it follows that $z_l=l(px/m)(k_{\|}/\omega)$, where $\omega=l\Omega_2$, and that

$$\mathscr{F}_{\|}(\omega/2\pi)=q^2\,k_{\|}^2\,\mathscr{V}(\omega/2\pi), \tag{2.37}$$

where $\mathscr{V}(\omega/2\pi)$ is the spectral density of $\varphi(s,t)$. The values of $k_{\|}$ appearing in (2.36) and (2.37) are related to ω by the dispersion relation appropriate to the wave mode in question.

Pitch-angle diffusion by bounce resonance has the distinctive property that particles having $x^2 \ll 1$ are much more strongly affected than those for which $x^2 \sim 1$. This means that bounce resonance may diffuse the mirror points of trapped particles to perhaps $\sim 20^\circ$ latitude from the magnetic equator, whereupon some complementary process, acting preferentially upon particles for which $x^2 \sim 1$, must complete the task of diffusing their equatorial pitch angles into the loss cone [43, 48].

II.5 Cyclotron Resonance

Particles that do not mirror at the equator often satisfy a resonance condition of the form

$$\omega - k_{\|}v_{\|} - l\Omega_1 = 0; \quad l = \pm 1, \pm 2, \ldots \tag{2.38}$$

with electromagnetic or electrostatic plasma cyclotron waves. This condition is known as Doppler-shifted local *cyclotron resonance*. If the wave frequency $\omega/2\pi$ is held constant, then $k_{\|}$ varies with position along the field line. Both $v_{\|}$ and Ω_1 vary with the position of a particle's guiding center in the course of its bounce motion. This is the sense in which cyclotron resonance is a *local* phenomenon; the conditions that satisfy (2.38) do not persist over the entire bounce path. Cyclotron resonances therefore have an intrinsic breadth $\Delta\omega=2\pi/\tau$, where the optimal interaction time τ is estimated from the expression

$$2\pi/\tau = \mathrm{Max}\,[\dot{\omega}\tau, (\ddot{\omega}/8)\,\tau^2] = \mathrm{Max}\,[(2\pi\dot{\omega})^{1/2}, (\pi^2\ddot{\omega}/2)^{1/3}]. \tag{2.39}$$

The symbols $\dot{\omega}$ and $\ddot{\omega}$ represent time derivatives of the value of ω required for resonance as the particle proceeds to execute its adiabatic bounce motion. Since $\dot{\omega}=0$ at the equator and at the mirror points, the optimal interaction time is then given by $\tau^3=16\pi/\ddot{\omega}$. Very roughly speaking, this means that $\Delta\omega \sim \varepsilon^{2/3}\Omega_1$. Local resonance, other than near points where $\dot{\omega}=0$, has an optimal interaction time given by $\tau^2=2\pi/\dot{\omega}$ and a minimum bandwidth $\Delta\omega \sim \varepsilon^{1/2}\Omega_1$. The case $\dot{\omega}=0$ appears somewhat the more favorable for sharp resonance, *i.e.*, for minimizing $\Delta\omega$.

Electrostatic Waves. Both of the above cases find τ to be substantially smaller than the bounce period (since $\varepsilon \ll 1$), and so the analytical problem can be treated in terms of a locally uniform **B** field. Diffusion of the local pitch angle α is equivalent to diffusion in x by virtue of (2.19). In a uniform **B** field containing only particles and electrostatic waves, the equation of motion for each Fourier component is

$$\dot{\mathbf{p}} + \Omega_1 (\mathbf{p} \times \hat{\mathbf{B}}) = q e_k \hat{\mathbf{k}} \exp(i\mathbf{k}\cdot\mathbf{r} - i\omega t + i\psi_k) \tag{2.40}$$

where $\Omega_1 = -qB/mc$. The component D_{xx} of the diffusion tensor [see (2.11)] is obtained from the local diffusion coefficient for $\cos\alpha \equiv p_\parallel/p$, where $p_\parallel = \mathbf{p}\cdot\hat{\mathbf{B}}$. There is no loss of generality in taking $k_x = 0$ and $k_y = k_\perp$ in the equation

$$\Delta(\cos\alpha)_k = \mathrm{Re} \int_0^\tau (q/p^3 k)\, e_k [p_\perp^2 k_\parallel - k_x p_\parallel p_x - k_y p_\parallel p_y] \times \exp(i k_x x + i k_y y + i k_\parallel z - i\omega t + i\psi_k)\, dt\,, \tag{2.41}$$

which follows from (2.40). Insertion of the unperturbed orbit $[x = (p_\perp c/qB)\cos(\Omega_1 t + \varphi_1);\ \ y = (p_\perp c/qB)\sin(\Omega_1 t + \varphi_1);\ \ z = v_\parallel t]$ then yields

$$\Delta(\cos\alpha)_k = \sum_{l=-\infty}^{+\infty} (q/p^3 k)\, e_k J_l(k_\perp p_\perp c/qB)[p_\perp^2 k_\parallel + l(qB/c)p_\parallel]\tau \cos(l\varphi_1 + \psi_k) \tag{2.42}$$

to the required first order of accuracy in e_k, upon application of (2.38). Evaluation of the phase averages over φ_1 and ψ_k finally implies

$$D_{xx} = \langle (B_e/B)(y/x)^2 (q^2/2p^2)\cos^2\alpha \times \sum_{l=-\infty}^{+\infty} J_l^2(k_\perp v_\perp/\Omega_1)\, \mathscr{V}(\omega/2\pi)[k_\parallel \sin\alpha - l(\Omega_1/v_\perp)\cos\alpha]^2 \rangle, \tag{2.43}$$

where the angle brackets denote a bounce average. The spectral density $\mathscr{V}(\omega/2\pi)$ is evaluated at the resonant ω given by (2.38) for each l. The weighted average over the various directions of $\hat{\mathbf{k}}$ present in the spectrum is tacitly understood in (2.43), as in (2.34).

The three remaining components of (2.11) do not vanish, but D_{xx} is the component of primary significance in the analysis of pitch-angle diffusion. Components such as D_{EE} and D_{xE} enable the waves to exchange energy with the particles. The direction of this energy exchange depends upon the form of the particle distribution function $\bar{f}(\mathbf{p},\mathbf{r})$, and leads accordingly either to amplification or attenuation of waves having a given value of $\mathbf{k}$ in the mode of interest. Thus, the free energy present in a non-Maxwellian particle distribution can be extracted by the available wave modes under certain conditions. This can lead to the spontaneous generation of plasma waves in the magnetosphere.

Electromagnetic Waves. The electromagnetic cyclotron modes of a plasma are of great geophysical interest in the context of spontaneous wave generation. For propagation along the magnetic field, these modes are circularly polarized, such that the magnetic-field perturbation is given by

$$b_x = b_\perp \cos(k_\parallel z - \omega t + \psi_k) \tag{2.44a}$$

$$b_y = \pm b_\perp \sin(k_\parallel z - \omega t + \psi_k)\,. \tag{2.44b}$$

Particles in a locally uniform unperturbed **B** field follow the equation of motion

$$\dot{\mathbf{p}} + \Omega_1 \mathbf{p} \times \hat{\mathbf{B}} = q\mathbf{e} + (q/mc)\mathbf{p} \times \mathbf{b} \tag{2.45}$$

when subjected to (2.44). The induced electric-field perturbation **e** is given by $n\mathbf{e} = -\hat{\mathbf{B}} \times \mathbf{b}$, where $n(\equiv ck_\parallel/\omega)$ is the refractive index.

If τ is the interaction time, then the first-order change in $\cos\alpha(\equiv p_\parallel/p)$ is given by

$$\Delta(\cos\alpha)_k = (q/np^2)[n(p/mc) - \cos\alpha] \int_0^\tau (p_x b_y - p_y b_x)\, dt = (q/np)[n(p/mc) - \cos\alpha]\, \tau b_\perp \sin\alpha \times \cos(\psi_k \mp \varphi_1);\ \ \omega - k_\parallel v_\parallel = \mp\Omega_1\,. \tag{2.46}$$

The upper sign in (2.44b) therefore leads to cyclotron resonance for $\omega - k_\parallel v_\parallel + \Omega_1 = 0$; the opposite polarization implies the resonance condition $\omega - k_\parallel v_\parallel - \Omega_1 = 0$. The required phase averages yield

$$D_{xx} = \langle (B_e/B)(y/x)^2 \cos^2\alpha (q^2/2n^2 p^2) \times [n(p/mc) - \cos\alpha]^2\, \mathscr{B}_\perp(\omega/2\pi) \rangle \tag{2.47}$$

upon application of (2.19), (1.22), and (1.05). The term np/mc dominates $\cos\alpha$ if $\omega \ll |\Omega_1|$, in which case the diffusion is approximately elastic ($\dot{p}_\parallel^2 \approx \dot{p}_\perp^2 \gg \dot{p}^2$).

It is instructive to recast the equation of motion as

$$p_\parallel \dot{p}_\parallel = q(p_\parallel/mc)(p_x b_y - p_y b_x) \tag{2.48a}$$

$$p_\perp \dot{p}_\perp = (q/n)[1 - (np_\parallel/mc)](p_x b_y - p_y b_x)\,. \tag{2.48b}$$

In terms of the phase velocity $v_p = \omega/k_\parallel$, it follows that

$$d(p^2)/dt = 2(mc/n)\dot{p}_\parallel = (v_p/v_\parallel)[d(p_\parallel^2)/dt] \tag{2.49a}$$

or

$$p_\perp^2 + 2\int (p_\parallel - m v_p) d p_\parallel = \text{constant} . \tag{2.49 b}$$

It is understood here that $\omega > 0$, that $\Omega_1 < 0$ for $q > 0$, and that $\Omega_1 > 0$ for $q < 0$. (This convention is not universally accepted.) The case $k_\parallel v_\parallel < 0$ corresponds to the normal Doppler shift (particle and wave traveling in opposite directions). It allows ions to resonate with ion-cyclotron waves (sometimes called LH for their left-handed polarization relative to **B**) and electrons to resonate with electron-cyclotron waves (otherwise known as RH or whistler-mode waves). According to (2.49), the wave gains energy from any resonant particle whose pitch angle thereby decreases. In other words, the conversion of $p_\perp^2$ into $p_\parallel^2$ is accompanied by the loss of particle energy to the wave, since $d(p^2)/dt < 0$ (see Fig. 19 [54]).

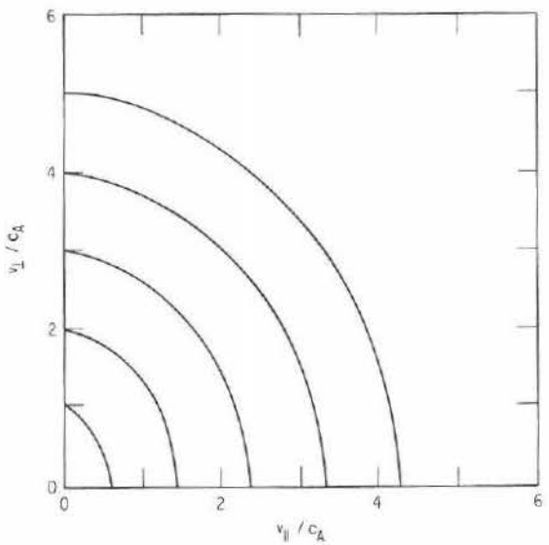

Fig. 19. Velocity-space trajectories of nonrelativistic protons resonant with electromagnetic proton-cyclotron waves propagating parallel to a uniform magnetic field [54].

Since pitch-angle diffusion tends to drive the distribution $\bar{f}$ toward pitch-angle isotropy, the anisotropy caused by the presence of a loss cone (see Section II.2) at $\alpha \approx 0$ represents a source of free energy for the amplification of ion- and electron-cyclotron waves. This is true because the pitch-angle diffusion produces a net diffusive flow of pitch

angles into the loss cone, thereby converting $p_\perp^2$ into $p_\parallel^2$ for the typical resonant particle[17].

For $k_\perp = 0$ the electromagnetic cyclotron modes in a cold plasma satisfy dispersion relations of the form

$$(c k_\parallel/\omega)^2 = 1 - \sum_j [\omega_j^2/\omega(\omega \pm \Omega_j)] \tag{2.50}$$

where the subscript j denotes particle species. The ion or electron plasma frequency $\omega_j/2\pi$ is given by $\omega_j^2 = 4\pi N_j q_j^2/m_j$, where N_j is the particle number density, q_j is the particle charge, and m_j is the particle rest mass. The nonrelativistic gyrofrequency $\Omega_j/2\pi$ is given by the formula $\Omega_j = -q_j B/m_j c$, so as to agree in sign with the definition of Ω_1 (see Section I.1; many authors define $\Omega_j \equiv +q_j B/m_j c$). The choice of sign in (2.50) depends upon the sense of circular polarization relative to **B**, as in (2.44). The upper sign corresponds to an ion-cyclotron mode, and the lower to an electron-cyclotron mode. In a two-component plasma ($j = e$ for electrons and $j = i$ for ions) it is customary to simplify (2.50) thus:

$$(c k_\parallel/\omega)^2 \approx \omega_e^2/\omega(\Omega_e - \omega); \qquad \omega \gg |\Omega_i| \tag{2.51 a}$$

$$(\omega/k_\parallel)^2 \approx c_A^2(1 - |\omega/\Omega_i|); \qquad \omega < |\Omega_i| . \tag{2.51 b}$$

The Alfvén speed $c_A \equiv (B^2/4\pi m_i N_i)^{1/2}$ is presumed to be much smaller than the speed of light c.

Various Types of Cyclotron Resonance. Resonance via the "normal" Doppler shift occurs for $k_\parallel v_\parallel = \omega - |\Omega_j/\gamma| < 0$. For electrons thus resonating with (2.51 a), the required whistler-mode wave frequency is related to the particle kinetic energy $(\gamma - 1) m_e c^2$ and local pitch angle α by

$$(c/c_A)^2 \cos^2\alpha = \frac{[1 - \gamma(\omega/\Omega_e)]^2 [1 - (\omega/\Omega_e)]}{(m_e/m_i)(\omega/\Omega_e)(\gamma^2 - 1)} . \tag{2.52 a}$$

For ions of velocity **v** resonating analogously with (2.51 b), the corresponding relationship is

$$\cos^2\alpha = \frac{(1 - |\gamma\omega/\Omega_i|)^2 (1 - |\omega/\Omega_i|)}{(v/c_A)^2 (\omega/\Omega_i)^2 \gamma^2} . \tag{2.52 b}$$

[17] A word of caution is in order here. The path along which particles diffuse in momentum space $(p_\parallel, p_\perp)$ is not a path of constant p. Thus, wave growth requires essentially that $-\nabla_p \bar{f}$ point toward increasing $p_\parallel$ (decreasing $p_\perp$) along the path of diffusion. This condition is somewhat more stringent than the minimal requirement of pitch-angle anisotropy [*i.e.*, $(\partial \bar{f}/\partial y)_E > 0$] at constant energy. A more quantitative stability analysis is given below (see Section II.6).

Figure 20 indicates the normalized frequency $|\omega/\Omega_j|$ required for resonance according to (2.52). The two cases of interest, electrons ($j=e$) resonating with (2.51a) and nonrelativistic ions ($j=i$) with (2.51b), are plotted separately.

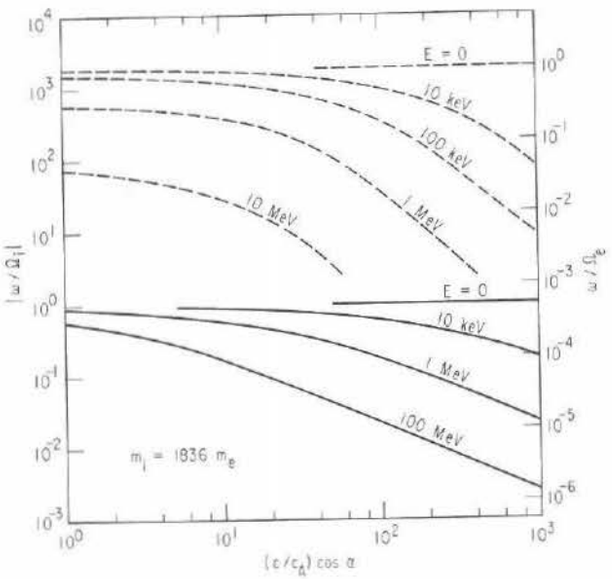

Fig. 20. Wave frequencies required for electromagnetic cyclotron resonance with protons (solid curves) and electrons (dashed curves) via the "normal" Doppler shift, assuming **k** parallel to **B**. Termination of electron-wave contours at $\omega\sim 2|\Omega_i|$ is dictated by use of (2.51a).

For a given particle, the minimum wave frequency $\omega/2\pi$ required for resonance is that required at the equator, where $v_{||}$ attains its maximum value and $|\Omega_j|$ its minimum along the bounce path. The distribution of particle density (hence, refractive index) along the field line cannot overcome this tendency unless B^2/N_j *decreases* with increasing B. Such a distribution of N_j occurs only in low-altitude regions where Coulomb collisions are already more important than wave-particle interactions in radiation-belt dynamics.

To the extent that $\mathscr{B}_\perp(\omega/2\pi)$ tends to fall with rising frequency in the resonant region, the "normal" Doppler-shifted cyclotron resonance acts preferentially upon particles that mirror away from the equator (see Fig. 20). This mechanism for pitch-angle diffusion is thus complementary to bounce resonance, which acts preferentially upon particles having

$x^2\ll 1$, in disposing of the particles that populate the earth's radiation belts [43].

A second form of cyclotron resonance involves the "overtaking" or "anomalous" Doppler shift ($k_{||}v_{||}=\omega+|\Omega_j/\gamma|>0$), whereby the particle sees a wave with its sense of circular polarization apparently reversed [50]. The "anomalous" Doppler shift enables ions to resonate with (2.51a) if

$$\cos^2\alpha\approx(c/nv)^2\approx(m_e/m_i)(\omega/\Omega_e)[1-(\omega/\Omega_e)](c_A/v)^2, \qquad (2.53\text{a})$$

where $n(\equiv ck_{||}/\omega)$ is the refractive index. Moreover, electrons can thus resonate with (2.51b)

$$(c/c_A)^2\cos^2\alpha\approx(\Omega_e/\omega)^2(\gamma^2-1)^{-1}(1-|\omega/\Omega_i|)^{-1}. \qquad (2.53\text{b})$$

This last interaction is believed to be responsible for the precipitation of relativistic electrons ($\gamma\gtrsim 4$) during the main and early recovery phases of a magnetic storm [51]. Figure 21 indicates the normalized wave frequencies $|\omega/\Omega_j|$ with which protons and electrons can resonate via the "anomalous" Doppler shift.

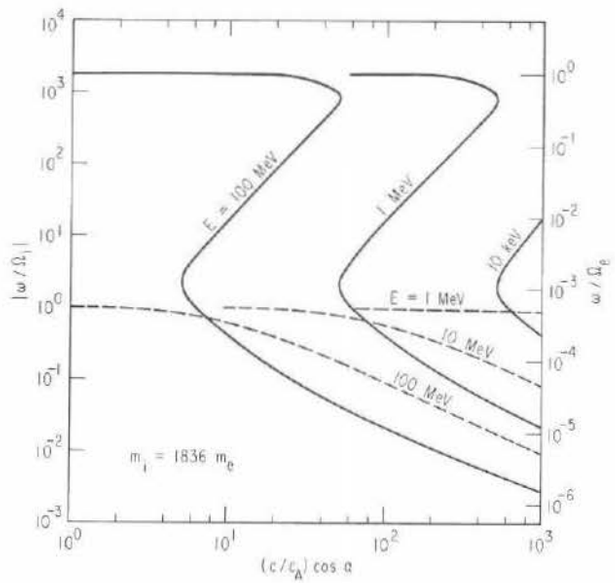

Fig. 21. Wave frequencies required for electromagnetic cyclotron resonance with protons (solid curves) and electrons (dashed curves) via the "anomalous" Doppler shift, assuming **k** parallel to **B**. Extension of proton contours to $\omega\lesssim|\Omega_i|$ is effected by using (2.50) in place of (2.51a).

For the pitch-angle anisotropy characteristic of a loss-cone distribution $\bar{f}$, the "anomalous" Doppler shift leads to a resonant pitch-angle diffusion that extracts energy from the wave spectrum. Moreover, the restriction that $k_\perp = 0$ makes (2.44)—(2.53) a somewhat oversimplified description of geophysical reality. The acceptance of $k_\perp \neq 0$ introduces cyclotron-harmonic resonances ($l \neq \pm 1$) accompanied by squared Bessel functions $J_l^2(k_\perp v_\perp/\Omega_1)$ in D_{xx}. Often these resonances also extract energy from the wave spectrum. Such wave-absorbing resonances are called *parasitic* [53], since they detract from the wave-amplifying properties of (2.52) in the presence of a loss-cone distribution. Ordinarily, however, the parasitic resonances account for only a fraction of the energy transfer between the particle distribution and wave spectrum, since they tend to be associated (at a given ω) with the more sparsely populated (high-energy) portion of $\bar{f}$ than the primary resonances described by (2.52). Thus, the wave-amplifying properties of $\bar{f}$ remain largely intact.

II.6 Limit on Trapped Flux

Plasma instabilities driven by radiation-belt particles are of special importance in that they can sometimes enforce an upper limit on the particle flux trapped by the geomagnetic field [52]. An instability analysis of the electromagnetic cyclotron modes is best formulated in terms of the plasma dielectric tensor derived from (1.12). The required operations can be simplified by taking $k_\perp = 0$, $e_\parallel = 0$, and

$$e_x = \pm i e_\perp \exp(i k_\parallel z - i\omega t + i\psi_k) \tag{2.54a}$$

$$e_y = e_\perp \exp(i k_\parallel z - i\omega t + i\psi_k)\,. \tag{2.54b}$$

The real part of (2.54) agrees with (2.44) if $e_\perp = -(\omega/ck_\parallel) b_\perp$. The Maxwell equations for this Fourier component of $\mathbf{e}$ and $\mathbf{b}$ thus read

$$\mathbf{k}\cdot\mathbf{e} = \mathbf{k}\cdot\mathbf{b} = 0\,, \tag{2.55a}$$

$$c\,\mathbf{k}\times\mathbf{e} = \omega\,\mathbf{b}\,, \tag{2.55b}$$

$$c\,\mathbf{k}\times\mathbf{b} = -4\pi i\mathbf{J} - \omega\,\mathbf{e}\,, \tag{2.55c}$$

where $\mathbf{J}$ is the current-density perturbation. The vanishing divergence of $\mathbf{e}$ is characteristic of the electromagnetic cyclotron wave modes at $k_\perp = 0$, since the perturbation of net charge density vanishes.

Dispersion Relation. It follows for these wave modes that

$$(c^2k^2 - \omega^2)\mathbf{e} = 4\pi i\omega\mathbf{J}\,. \tag{2.56}$$

If the distribution function $f_j(\mathbf{p},\mathbf{r};t)$ for species j is decomposed into a phase-averaged part $\bar{f}_j(\mathbf{p},\mathbf{r})$ plus an oscillatory part $\tilde{f}_j(\mathbf{p},\mathbf{r};t)$, the Vlasov equation (1.12) can be written in the linearized form

$$\begin{aligned} &-i(\omega - k_\parallel v_\parallel)\tilde{f}_j - (\Omega_j/\gamma_j)\mathbf{p}\times\hat{\mathbf{B}}\cdot\nabla_p\tilde{f}_j \\ &= -q_j\mathbf{e}\cdot\nabla_p\bar{f}_j - q_j(k_\parallel/\omega)\mathbf{v}\times(\hat{\mathbf{k}}\times\mathbf{e})\cdot\nabla_p\bar{f}_j \\ &= -(q_j/\omega)(\omega - k_\parallel v_\parallel)\mathbf{e}\cdot\nabla_p\bar{f}_j - q_j(k_\parallel/\omega)(\mathbf{e}\cdot\mathbf{v})(\partial\bar{f}_j/\partial p_\parallel)\,, \end{aligned} \tag{2.57}$$

where γ_j is the ratio of relativistic mass to rest mass. By transforming to the variables $p_\perp$ and φ_1, such that $p_x = -p_\perp\sin\varphi_1$ and $p_y = p_\perp\cos\varphi_1$ during unperturbed gyration, it can be shown that

$$\begin{aligned} &(\Omega_j/\gamma_j)(\partial\tilde{f}_j/\partial\varphi_1) - i(\omega - k_\parallel v_\parallel)\tilde{f}_j \\ &\quad = -\left[(q_j/\omega p_\perp)(\omega - k_\parallel v_\parallel)(\partial\bar{f}_j/\partial p_\perp)\right. \\ &\qquad \left. + (q_j k_\parallel/\gamma_j m_j\omega)(\partial\bar{f}_j/\partial p_\parallel)\right](e_x p_x + e_y p_y) \\ &\qquad + (q_j/\omega p_\perp^2)(\omega - k_\parallel v_\parallel)(\partial\bar{f}_j/\partial\varphi_1)(e_x p_y - e_y p_x)\,. \end{aligned} \tag{2.58}$$

The final line of (2.58) vanishes because $\bar{f}_j$ is phase-averaged, and therefore independent of φ_1.

It is assumed that ω has a small imaginary part that describes the damping ($\mathrm{Im}\,\omega < 0$) or growth ($\mathrm{Im}\,\omega > 0$) of the wave. It is proper to view (2.58) as an ordinary differential equation for $\tilde{f}_j(\varphi_1)$, subject to the "boundary" condition that $\tilde{f}_j(-\infty) = 0$ for $\mathrm{Im}\,\omega > 0$ and $\tilde{f}_j(+\infty) = 0$ for $\mathrm{Im}\,\omega < 0$. Thus, the solution of (2.58) may be written

$$\begin{aligned} \tilde{f}_j(\varphi_1) = (q_j/2\omega)&\left[(\omega - k_\parallel v_\parallel)(\partial\bar{f}_j/\partial p_\perp) + k_\parallel v_\perp(\partial\bar{f}_j/\partial p_\parallel)\right] \\ &\times\left[\frac{(e_x - ie_y)\exp(i\varphi_1)}{\omega - k_\parallel v_\parallel - (\Omega_j/\gamma_j)} - \frac{(e_x + ie_y)\exp(-i\varphi_1)}{\omega - k_\parallel v_\parallel + (\Omega_j/\gamma_j)}\right]. \end{aligned} \tag{2.59}$$

The electric current-density perturbation $\mathbf{J}$ can thus be written

$$\begin{aligned} \mathbf{J} &= \sum_j q_j\int v_\perp(\hat{\mathbf{y}}\cos\varphi_1 - \hat{\mathbf{x}}\sin\varphi_1)\tilde{f}_j(\varphi_1)\,d^3p \\ &= \sum_j (q_j^2/2i\omega)\,\mathbf{e}\int\frac{\left[(\omega - k_\parallel v_\parallel)(\partial\bar{f}_j/\partial p_\perp) + k_\parallel v_\perp(\partial\bar{f}_j/\partial p_\parallel)\right]v_\perp\,d^3p}{\omega - k_\parallel v_\parallel \pm(\Omega_j/\gamma_j)} \end{aligned} \tag{2.60}$$

where $d^3p = p_\perp\,dp_\perp\,dp_\parallel\,d\varphi_1$, and where the choice of sign ($\pm$) corresponds to the choice of polarization ($e_x = \pm ie_y$) in (2.54). In terms of the unit-normalized distribution function $F_j = N_j^{-1}\bar{f}_j$, the dispersion relation deduced from (2.56) for $k_\perp = 0$ is therefore

$$c^2k^2 = \omega^2 + \pi\sum_j\omega_j^2 I_j\,, \tag{2.61a}$$

where

$$\int_{-\infty}^{+\infty}\int_{0}^{\infty}\frac{[(\omega-k_{\|}v_{\|})(\partial F_j/\partial p_\perp)+k_{\|}v_\perp(\partial F_j/\partial p_{\|})]\,p_\perp^2\,dp_\perp\,dp_{\|}}{\gamma_j(\omega-k_{\|}v_{\|})\pm\Omega_j}. \quad (2.61\,b)$$

In the rest frame of a cold plasma whose various components j exhibit no relative streaming along **B**, the integration of each I_j by parts allows (2.50) to be recovered from (2.61).

Growth Rate. If the cold plasma is augmented by a comparatively *small* density of hot plasma or of radiation-belt particles, then (2.50) remains approximately valid for relating $k_{\|}$ to the real part of ω. The growth rate $\mathrm{Im}\,\omega$ follows directly from (2.61). If $\nabla_p\bar{f}$ is free of substantial variation in the velocity interval extending $\sim|(3\,\mathrm{Im}\,\omega/k_{\|})|$ to either side of the resonant velocity $v_r\equiv(\omega/k_{\|})\pm(\Omega_j/\gamma_j k_{\|})$, then the integral over $p_{\|}$ can be simplified by means of the formula

$$[\gamma_j(\omega-k_{\|}v_{\|})\pm\Omega_j]^{-1}\approx\mathrm{P}\{[\gamma_j(\omega-k_{\|}v_{\|})\pm\Omega_j]^{-1}\}-i\pi m_j|k_{\|}|^{-1}\delta(p_{\|}-\gamma_j m_j v_r), \quad (2.62)$$

where P denotes the Cauchy principal value and δ the Dirac function. It follows that

$$c^2k^2\approx\omega^2-\sum_j[\omega_j^2\,\omega/(\omega\pm\Omega_j)]-4\pi^3 i|k_{\|}|^{-1}\sum_j q_j^2\int_0^\infty[\mp(\Omega_j/\gamma_j)(\partial\bar{f}_j/\partial p_\perp)+k_{\|}v_\perp(\partial\bar{f}_j/\partial p_{\|})]\,p_\perp^2\,dp_\perp, \quad (2.63)$$

where the integral follows the path $p_{\|}=\gamma_j m_j(\omega/k_{\|})\mp(q_jB/ck_{\|})$.

It is inconvenient to evaluate (2.63) in its full relativistic generality. Since the resonant protons and electrons that tend to amplify magnetospheric cyclotron waves are typically nonrelativistic, it is reasonable to adopt the nonrelativistic ($\gamma_j=1$) approximation for evaluating (2.63), in which case the integral follows a path of constant $p_{\|}$. In this approximation, a particle distribution whose energy spectrum follows a power law (E^{-l}) and whose pitch-angle distribution approximates $\sin^{2s}\alpha$ over the unit sphere (l and s are not necessarily integers) may be represented as

$$\bar{f}_j(\mathbf{p},\mathbf{r})=(p_j/p)^{2l}(p_\perp/p)^{2s}p^{-2}J_\perp(p_j^2/2m_j), \quad (2.64)$$

where p_j is the scalar momentum that corresponds to a kinetic energy $p_j^2/2m_j$. The form of $\bar{f}_j$ given by (2.64) is observationally realistic, as well as algebraically convenient. It leads (2.63) to predict a growth

rate $\mathrm{Im}\,\omega$, given in lowest order by taking the imaginary part of (2.63). The result is

$$\mathrm{Im}\,\omega\approx-4\pi^3|k_{\|}|^{-1}\sum_j q_j^2(p_j/m_j v_r)^{2l}\,\mathrm{B}(s+1,l)[\omega+s(\omega\pm\Omega_j)]J_\perp(p_j^2/2m_j)\div\{2\omega\mp\sum_j[\omega_j^2\,\Omega_j/(\omega\pm\Omega_j)^2]\}, \quad (2.65)$$

where $\mathrm{B}(s+1,l)\equiv\Gamma(s+1)\Gamma(l)/\Gamma(s+l+1)$ is the beta function. The denominator of (2.65) can be expressed as $2\omega(c^2/v_pv_g)$, where $v_p(=\omega/k_{\|})$ and $v_g(=d\omega/dk_{\|})$ respectively represent the phase and group velocities of the wave in the direction of **B**.

If parasitic resonances (see Section II.5) are neglected, as is usually permissible in the magnetosphere, the growth rate

$$\mathrm{Im}\,\omega\approx-(2\pi^3/\omega)(v_gv_p/c^2)|k_{\|}|^{-1}q_j^2(p_j/m_jv_r)^{2l}\times\mathrm{B}(s+1,l)[\omega+s(\omega-|\Omega_j|)]J_\perp(p_j^2/2m_j) \quad (2.66)$$

thus follows from the interaction of electrons with the whistler mode ($j=e$) or from the interaction of protons with the proton-cyclotron mode ($j=i$). The growth rate is therefore positive at frequencies such that $0<\omega<|s\Omega_j/(s+1)|$. Since (2.66) is based on the dynamics of an infinite homogeneous plasma, however, a positive value of $\mathrm{Im}\,\omega$ is not synonymous with an instability that spontaneously generates appreciable wave intensity in the magnetosphere. Instability in this latter sense requires at least a small coefficient R of internal reflection, as in a maser, to prevent all the wave energy from escaping [52]. If the typical path length between the points of wave reflection is $\sim La$, then the condition for spontaneous wave generation (maser action) is

$$2La\,\mathrm{Im}\,\omega>|v_g\ln R|. \quad (2.67)$$

This condition imposes an upper limit on the particle flux that the magnetosphere can stably contain. Instability in the sense of (2.67) generates wave energy that, by virtue of (2.47), causes the pitch angles of the excess particles to diffuse into the loss cone until (2.67) is no longer satisfied [52].

Limiting Flux. The upper limit on stably trapped particle flux is customarily expressed as a bound on the integral omnidirectional flux

$$I_{4\pi}(p_j^2/2m_j)=4\pi\int_0^1\sin^{2s}\alpha\,d(\cos\alpha)\int_{p_j^2/2m_j}^\infty J_\perp(p_j^2/2m_j)(p_j/p)^{2l}\,dE=[\pi^{3/2}(p_j^2/m_j)\Gamma(s+1)/(l-1)\Gamma(s+\tfrac{3}{2})]J_\perp(p_j^2/2m_j) \quad (2.68)$$

above the minimum particle energy with which a wave having $\mathrm{Im}\,\omega>0$ can resonate, *i.e.*, for a value of p_j given by $p_j^*=(m_j/k_{\|})(\omega-|\Omega_j|)$, where $\omega=|s\Omega_j/(s+1)|$. The critical nonrelativistic particle energies for electrons resonant with (2.51a) and protons resonant with (2.51b) are therefore given respectively by

$$E^*=B^2/8\pi N_e(s+1)^2 s \tag{2.69a}$$

$$E^*=B^2/8\pi N_p(s+1)s^2. \tag{2.69b}$$

An estimate for the critical (maximum) value of $I_{4\pi}(E^*)$ is obtained from (2.66)—(2.68) by replacing $\omega+s(\omega-|\Omega_j|)$ with the value that maximizes $\mathrm{Im}\,\omega/v_g$. This prescription tacitly ignores any frequency dependence of $\ln R$, *i.e.*, it is assumed that the internal-reflection coefficient is independent of wave frequency over the band of interest. It is thus estimated that $\mathrm{Im}\,\omega/v_g$ peaks at

$$\omega+s(\omega-|\Omega_j|)\approx-(s/2)|\Omega_j|\left[(l-1)(v_p/v_g)+sl\right]^{-1} \tag{2.70}$$

if $sl+(l-1)(v_p/v_g)\gg 1/2$.

If the particle spectrum is at least moderately steep ($l\gtrsim 4$), then the value of $\mathrm{Im}\,\omega/v_g$ does in fact descend sharply from a peak [where ω is given by (2.70)] to zero [where $\omega=|s\Omega_j/(s+1)|$], as required. The limiting flux is then given by

$$I_{4\pi}^*(E^*)\approx\frac{\{(v_p/v_g)+[sl/(l-1)]\}\,cB\Gamma(l+s+1)|\ln R|}{2\pi^{3/2}|q_j|(s+1)^2 s\Gamma(l)\,\Gamma(s+\frac{3}{2})La}, \tag{2.71}$$

with v_p/v_g evaluated at $\omega+s(\omega-|\Omega_j|)=0$: thus $v_p/v_g=(s+1)/2$ for electrons and $1+(s/2)$ for protons. For practical application, it is usual to insert apparently reasonable values of the various parameters (*e.g.*, $v_p/v_g\sim 1$, $l\sim 4$, $s\sim 1/2$, $\ln R\sim -3$) and to cite a common upper bound

$$I_{4\pi}^*(E^*)\sim(10^{11}/L^4)\,\mathrm{cm}^{-2}\,\mathrm{sec}^{-1} \tag{2.72}$$

for the *equatorial* integral omnidirectional flux of stably trapped particles (either electrons or protons, separately) exceeding the appropriate critical energy given by (2.69).

Observational evidence for such a limit on the flux of trapped electrons is shown in Fig. 22. For $s\sim 1/2$, the value of E^* given by (2.69a) approximates the magnetic energy per *plasma* electron (≈ 40 keV if $N_e\approx 4\,\mathrm{cm}^{-3}$ at $L=5$). Data points representing the omnidirectional flux of electrons greater than 40 keV in energy are distributed generally below $I_{4\pi}^*$ on the logarithmic scale; the flux exceeds $I_{4\pi}^*$ only in isolated (unstable) instances (see also Section IV.4).

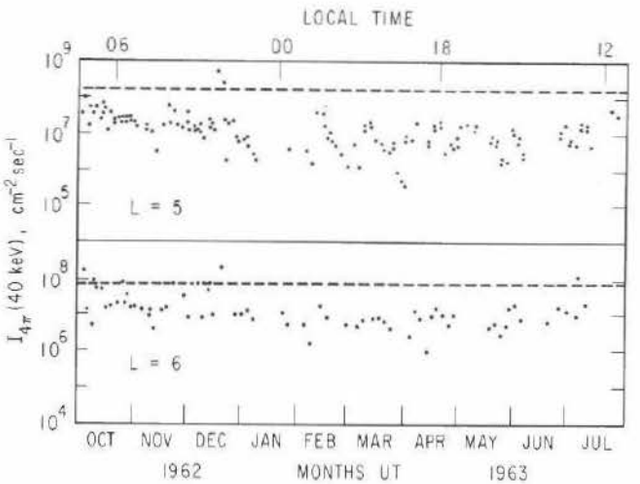

Fig. 22. Compilation of near-equatorial electron-flux measurements (magnetic latitudes $<30^\circ$ at $L=5$ and $<15^\circ$ at $L=6$) from Explorer 14 [52].

II.7 Weak Diffusion and Strong Diffusion

Although some degree of inelasticity is essential for wave growth or damping, cyclotron-resonant interactions of energetic (radiation-belt) particles are often preponderantly elastic in the sense that $D_{EE}\ll E|D_{xE}|\ll E^2 D_{xx}$. This property has been illustrated schematically in Fig. 19. The degree of inelasticity is of order $(\gamma_j\omega/\Omega_j)^2$ in the electromagnetic case, and the more energetic particles tend to resonate (Figs. 20—21) with the lower-frequency waves. Thus, the Jacobian given by (2.14) remains approximately applicable to the cyclotron-resonant pitch-angle diffusion of radiation-belt particles, and the equation

$$\frac{\partial\bar{f}}{\partial t}=\frac{1}{x\,T(y)}\frac{\partial}{\partial x}\left[x\,T(y)\,D_{xx}\frac{\partial\bar{f}}{\partial x}\right] \tag{2.73}$$

approximates their dynamical behavior at constant energy.

Since $T(y)$ varies only moderately with $y\equiv(1-x^2)^{1/2}$, the solutions of (2.73) must somewhat reesemble those for symmetric diffusion in a cylinder. If D_{xx} is approximately constant in x, the decaying eigenfunctions of pitch-angle diffusion must then resemble the sequence

$\exp[-D_{xx}(\kappa_n/x_c)^2 t]\,J_0(\kappa_n x/x_c)$ in order to satisfy the boundary condition[18] that $\bar{f}=0$ at $x=x_c$ [43]. Here the κ_0 (≈ 2.40), κ_1 (≈ 5.52), κ_2 (≈ 8.65), *etc.*, denote the roots of the Bessel function $J_0(x)$ in ascending sequence. This means that a suddenly injected distribution of trapped particles settles toward the lowest eigenmode of pitch-angle diffusion at the *e*-folding rate $\sim(\kappa_1^2-\kappa_0^2)(D_{xx}/x_c^2)$ upon removal of the particle source. Once the lowest eigenmode is attained, the pitch-angle distribution ceases to change its functional form, but proceeds to decay exponentially in time at a rate $\sim\kappa_0^2(D_{xx}/x_c^2)$. The characteristic lifetime of a particle against pitch-angle diffusion into the loss cone, *i.e.*, the *e*-folding time for the lowest eigenmode, thus exceeds by a factor ~ 4 the time required for attaining the lowest normal mode from an initially abnormal distribution of pitch angles (see Section IV.2).

A pitch-angle distribution of the form y^{2s} (see Section II.6) yields a decay rate of $4sD_{xx}$ at $x=0$ in either (2.35) or (2.73). If $x_c^2 s\sim 1$, this rate is quite comparable to the estimate $\kappa_0^2(D_{xx}/x_c^2)$ based on the cylinder analogy (see above). For comparison, the lowest eigenvalue of (2.20) is $(\pi^2/4)(D_{\xi\xi}/\xi_c^2)$ if $\bar{f}$ is required to vanish at $\xi=\pm\xi_c$. The numerical consistency of these estimates enables the particle lifetime to be characterized as $x_c^2/5D_{xx}$, within perhaps a factor of two.

The above considerations apply to a condition known as *weak diffusion*, in which the lifetime $x_c^2/5D_{xx}$ is sufficiently long compared to the bounce period $2\pi/\Omega_2$. The reason for this cautious interpretation is that the dense atmosphere is typically distant from the site of pitch-angle diffusion caused by a wave-particle interaction. Thus, the diffusing particles are unaware of a loss cone in momentum space (see Fig. 19) until they attempt to enter the dense atmosphere in the subsequent course of bounce motion. The requirement for applying (2.73) with the boundary condition that $\bar{f}=0$ at $x=\pm x_c$ amounts to the demand that

$$(\pi/\Omega_2)D_{xx}\ll(1-x_c)^2. \tag{2.74}$$

This means that a typical particle originating at $x=\pm x_c$ must be unable to wander (diffuse) across any substantial fraction of the loss-cone aperture during a single pass between mirror points. If (2.74) fails to hold, then the boundary condition that $\bar{f}=0$ at $x=\pm x_c$ applies only to upward-bound particles between the dense atmosphere and the site of pitch-angle diffusion, not to the entire bounce orbit. In such a case, the analysis based on (2.73) must take account of the substantial probability that a particle's pitch angle may wander into and back out of the loss

[18] This discussion is facilitated by the tacit assumption of a centered-dipole field, for which the loss-cone angle does not vary with longitude. The generalization to an offset-dipole model is indicated below.

cone (perhaps several times) during a single transit of the (typically equatorial) region where the wave-particle interaction occurs.

The foregoing considerations are based on the tacit assumption of a centered-dipole field. When the eccentricity of the dipole is taken into account, it is necessary to distinguish between the *bounce loss cone*, which contains particles that will *precipitate* (lose their energy to the dense atmosphere) within one bounce period, and the *drift loss cone*, whose aperture is given by (2.24). The aperture of the bounce loss cone varies with azimuth, and attains its maximum (identical with the aperture of the drift loss cone) near the South Atlantic "anomaly". Particles within the drift loss cone, but outside the local bounce loss cone, proceed to drift in azimuth but are doomed to precipitate somewhat prior to visiting the "anomaly".

An estimate for the bounce loss-cone angle $\cos^{-1}x_b$ follows from generalizing (2.24) to arbitrary longitude φ relative to the "anomaly", where $\varphi=\varphi_a$. The result, *viz.*,

$$\begin{aligned}1-x_b^2\approx{}&[(a+h)/La]^3[1+3r_0(La)^{-1/2}(a+h)^{-1/2}\cos(\varphi-\varphi_a)]\\&\div[4-(3/La)(a+h)-3r_0(La)^{-3/2}(a+h)^{1/2}\cos(\varphi-\varphi_a)]^{1/2},\end{aligned} \tag{2.75}$$

suggests a rather pronounced azimuthal modulation of the aperture of the bounce loss cone[19] at $L\lesssim 3$. As a result, particle precipitation tends to concentrate in azimuth near (slightly prior to) the "anomaly" in the absence of a counteracting variation of D_{xx} with φ (see Section IV.2). Since the meaning of (2.74) is somewhat ambiguous under azimuthal asymmetry, it is customary to regard *weak diffusion* as a condition applicable to any longitude at which

$$(\pi/\Omega_2)D_{xx}\ll(1-x_b)^2. \tag{2.76}$$

In the opposite extreme, if $D_{xx}\gg(\Omega_2/\pi)$, then the distribution $\bar{f}$ is immune from boundary conditions in x throughout the region in which pitch-angle diffusion occurs. On a single pass through this scattering region, a particle's probable pitch angle becomes thoroughly randomized over the unit sphere. This condition, known as *strong diffusion* [53], causes $\bar{f}$ to exhibit virtual isotropy in pitch angle within the scattering region. In the limit of strong diffusion, the decay rate of $\bar{f}$ is limited not by the magnitude of D_{xx} (of which $\partial\bar{f}/\partial t$ is actually independent), but rather by the solid angle of the bounce loss cone and by the bounce frequency $\Omega_2/2\pi$. Under strong diffusion, a fraction $1-x_b$ of

[19] Thus, x_c is defined as the maximum value attained by the azimuthally varying parameter x_b.

the trapped particles will precipitate during each half bounce period, since the solid angle of either bounce loss cone is $2\pi(1-x_b)$. The loss rate is therefore given by

$$\lambda = -\partial \ln \bar{f}/\partial t = (\Omega_2/\pi)(1-x_b) \tag{2.77}$$

in the limit of strong diffusion. This limit represents an ultimate standard by which all diffusive precipitation mechanisms can be judged for effectiveness. Several storm-associated phenomena (*e.g.*, ring-current, relativistic-electron, and auroral precipitation) are actually observed to approximate the limit of strong diffusion [51, 52, 54].